

Many-body localization with synthetic gauge fields in disordered Hubbard chains

Kuldeep Suthar,¹ Piotr Sierant,^{1,2} and Jakub Zakrzewski^{1,3}

¹*Instytut Fizyki im. Mariana Smoluchowskiego, Uniwersytet Jagielloński, Łojasiewicza 11, 30-348 Kraków, Poland*

²*ICFO- Institut de Sciences Fotoniques, The Barcelona Institute of Science and Technology, 08860 Castelldefels (Barcelona), Spain*

³*Mark Kac Complex Systems Research Center, Uniwersytet Jagielloński, Kraków, Poland. **

(Dated: December 21, 2024)

We analyze the localization properties of the disordered Hubbard model in the presence of a synthetic magnetic field. An analysis of level spacing ratio shows a clear transition from ergodic to many-body localized phase. The transition shifts to larger disorder strengths with increasing magnetic flux. Study of dynamics of local correlations and entanglement entropy indicates that charge excitations remain localized whereas spin degree of freedom gets delocalized in the presence of the synthetic flux. This residual ergodicity is enhanced by the presence of the magnetic field with dynamical observables suggesting incomplete localization at large disorder strengths. Furthermore, we examine the effect of quantum statistics on the local correlations and show that the long-time spin oscillations of a hard-core boson system are destroyed as opposed to the fermionic case.

I. INTRODUCTION

The phenomenon of many-body localization (MBL) has attracted a significant interest in condensed matter physics over past several years, both theoretically [1–4] and experimentally [5–9]. The MBL is an extension of Anderson localization (which describes localization of single-particle eigenstates in the presence of disorder potential) to highly excited eigenstates of interacting many-body systems. The characteristic properties of MBL phase are Poisson eigenvalue statistics [10–16], an absence of thermalization [17–20], a vanishing transport [21–23], and the logarithmic spreading of the entanglement entropy [24–26]. Starting from early works, many aspects of the topic have been examined to date. The ultracold atomic systems are ideal platform to explore the localization phenomena due to their ability to tune dimensionality, nature of applied disorder, atomic interactions, lattice geometry and synthetic gauge fields. The existence of MBL phase has been confirmed in recent quantum gas experiments using quantum simulators such as optical lattices [5, 6, 27, 28] and trapped ions [8]. Moreover, the flux dependent mobility edge of disordered chain and the significance of symmetry on the localization and transport properties in the presence of synthetic gauge field have been explored in experiments [29, 30].

The nonergodic behaviour of disorder Hubbard chain at strong disorder and temporal evolution of its correlation functions have been examined theoretically in [26, 31]. The SU(2) symmetry of the model limits the full MBL as the charge degrees of freedom are localized but spins remain delocalized and reveal subdiffusive dynamics [32–34]. The partial MBL is due to the separation of time scale between charge and spin sectors in the presence of correlated disorder [35] and the decay rate of the transport strongly depends on the density of singly occupied sites in the initial state [36]. The implementation of synthetic gauge field in ultracold atoms and recently on disorder systems allows one to study the effect of time-reversal symmetry breaking on the localization properties of the disordered fermions [29, 37]. Furthermore, it is possible

to couple internal atomic spin states which allows for an interpretation in terms of an additional synthetic lattice dimension [38, 39]. The gauge field in synthetic dimension leads to flux ladders where the hopping and atomic interactions between different states can be controlled in experiments [40]. The presence of the random gauge fields delocalizes the interacting system [41] and many-body states become extended into a single Landau level [42]. Despite numerous studies on the topic of MBL, the effects of time-reversal symmetry breaking on localization phenomena have been sparsely studied [43] and this is the subject of the present study.

In particular, we examine the spectral and dynamical properties of disordered Hubbard chains in the presence of the synthetic gauge fields. At lower disorder strengths, in ergodic regime, the breaking of time-reversal invariance (TRI) by gauge field results in spectral statistics well described by Gaussian Orthogonal Ensemble (GOE) of random matrices instead of Gaussian Unitary Ensemble (GUE) as expected for broken TRI. This is due to a residual discrete symmetry. Only when the residual reflection symmetry is broken by local field or asymmetric tunneling rate of spin-up and down fermions, the level statistics is characterized by GUE. The time dynamics of charge and spin correlations for random initial states reveal the localization of charges and a subdiffusive decay of spin correlations. The introduction of a synthetic flux damps the spin oscillations and finally delocalizes them. Furthermore, the entanglement entropy confirms the delocalization of spins in the presence of the synthetic gauge fields.

The paper is organized as follows. In Sec. II we introduce the Hubbard model with synthetic gauge field and disorder. In Sec. III we analyze the effect of symmetry breaking and synthetic flux on the spectral properties of the system. We further study the local charge and spin dynamics of fermions and hard-core bosons in Sec. IV. In Sec. V we examine the bipartite entanglement entropy. The local correlations in the presence of spin-dependent disorder are discussed in Sec. VI. Finally, we conclude in Sec. VII.

* jakub.zakrzewski@uj.edu.pl

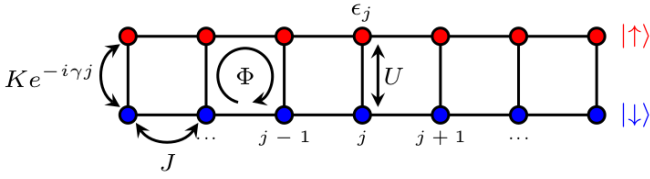


FIG. 1. Schematic visualization of the system studied (1) in which up (down)-spin corresponds to upper (lower) rung of the ladder.

II. THE MODEL

We consider interacting spin-1/2 fermions in a quasi-one dimensional lattice. The two spin components can be interpreted as the realization of a two-leg ladder geometry, with two legs corresponding to two spin states. Two components may be realized as in the recent experiment [5] for ^{40}K atoms with spin up state being $|F, m_F\rangle = |\frac{9}{2}, -\frac{7}{2}\rangle \equiv |\uparrow\rangle$ and the spin-down state $|\frac{9}{2}, -\frac{9}{2}\rangle \equiv |\downarrow\rangle$. The two spin components may be coupled by e.g. Raman coupling realizing the Hamiltonian [39, 44] $\hat{H} = \hat{H}_0 + \hat{H}_{\text{sb}}$, wherein

$$\begin{aligned} \hat{H}_0 = & - \sum_{j,\sigma} \left(J \hat{c}_{j,\sigma}^\dagger \hat{c}_{j+1,\sigma} + K e^{-i\gamma j} \hat{c}_{j,\uparrow}^\dagger \hat{c}_{j,\downarrow} + \text{H.c.} \right) \\ & + U \sum_j \hat{n}_{j,\uparrow} \hat{n}_{j,\downarrow} + \sum_{j,\sigma} \epsilon_j \hat{n}_{j,\sigma}. \end{aligned} \quad (1)$$

Here, j and $\sigma = \uparrow, \downarrow$ are the spatial and spin indices, J is the hopping amplitude between neighbouring lattice sites on the same leg and K is the strength of complex hopping in the synthetic dimension, $\hat{c}_{j,\sigma}^\dagger$ ($\hat{c}_{j,\sigma}$) creates (annihilates) fermions with spin σ at site j , and the occupation number operator $\hat{n}_{j,\sigma} = \hat{c}_{j,\sigma}^\dagger \hat{c}_{j,\sigma}$. The local “charge” density is $n_j = n_{j,\uparrow} + n_{j,\downarrow}$ while the spin magnetization is $m_j = n_{j,\uparrow} - n_{j,\downarrow}$. The on-site interaction strength of two spins is assumed to be repulsive i.e. $U > 0$ and ϵ_j is the uniform distributions of a random spin-independent on-site potential, $\epsilon_j \in [-W/2, W/2]$ with W being the disorder amplitude. The parameter $\gamma = 2k_R a$ determines the synthetic magnetic flux with the flux per plaquette of the lattice being $\Phi = \gamma/2\pi$. Here k_R is the recoil wave vector of the Raman beams and a is the lattice spacing [44]. The finite value of γ leads to complex hoppings along the rungs of the ladder (corresponding to flipping the spins). The system length along the synthetic dimension is two, although it may be increased by trapping few Fermi mixtures together. The gauge is chosen in such a way that the Peierls phase is along the rung and not on the legs of the ladder - compare Fig. 1. The above model Hamiltonian without a synthetic gauge field has been realized in quantum gas experiments in optical lattices [5] similarly physics with the synthetic dimension in clean, disorder-free experiments has also been studied [40].

The hopping amplitude sets the unit of energy scale, $J = 1$ and we use periodic boundary conditions throughout this work. We study the system at unit filling (the total number of fermions $N = N_\uparrow + N_\downarrow = 1$ is conserved). Note that such a

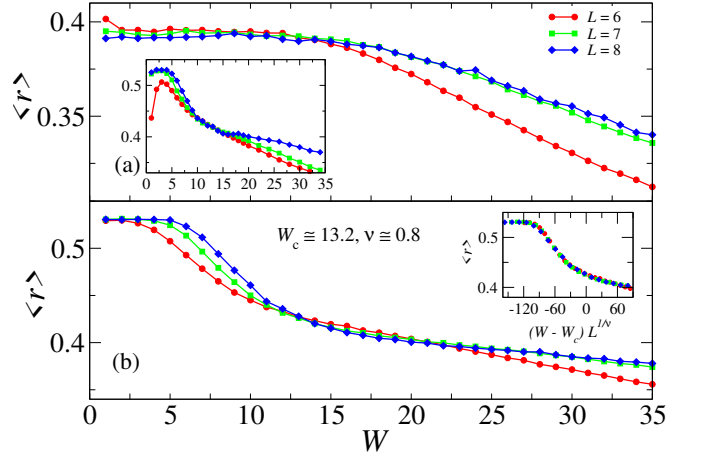


FIG. 2. Mean gap ratio $\langle r \rangle$ around the center of the spectra $\epsilon \approx 0.5$ as a function of disorder strength W for TRI case of $K = 1$, $\gamma = 0$ of Hamiltonian (1) in the absence (a) or in the presence (b) of the symmetry breaking local term (2) for $h_b = 0.5$. The overlapping distinct spectra in case (a) lead to almost Poissonian level statistics for any W (main figure). The inset in (a) shows that diagonalization of a single symmetry block of the Hamiltonian allow to observe the crossover between GOE-like behavior at low W to Poisson statistics for larger W . The inset in panel (b) shows the finite size scaling of the data yielding the critical disorder strength and exponent of ergodic to MBL phase transition. The number of disorder realizations considered are 5000, 2000, and 500 for the system size $L = 6, 7$, and 8, respectively.

situation is sometimes called a half-filling in condensed matter community. In the absence of the gauge field ($K = 0$), the model Hamiltonian preserves parity, time-reversal and $\text{SU}(2)$ spin symmetry [45], however, pseudospin $\text{SU}(2)$ [46] and particle-hole symmetries are broken due to the on-site disorder potential. The parity and $\text{SU}(2)$ spin symmetry can be removed by adding a local weak magnetic field (h_b) at the edge of the chain [26]. The symmetry breaking Hamiltonian is

$$\hat{H}_{\text{sb}} = h_b (\hat{n}_{1,\uparrow} - \hat{n}_{1,\downarrow}). \quad (2)$$

Additionally, the presence of gauge field in the synthetic dimension breaks the time-reversal symmetry of the system.

We use an exact diagonalization for different system size and flux quanta obtaining both spectral and time evolution properties of systems studied. While using more sophisticated techniques one could extend the study to slightly larger systems, we restrict ourselves in this exploratory approach to small $L \leq 8$ system amenable to exact diagonalization. We estimate influence of finite size effects on our results by comparison with smaller system sizes. While the question of a possible instability of MBL phase in thermodynamic limit is debated [47–50], we believe that our results are robust on experimentally relevant time scales.

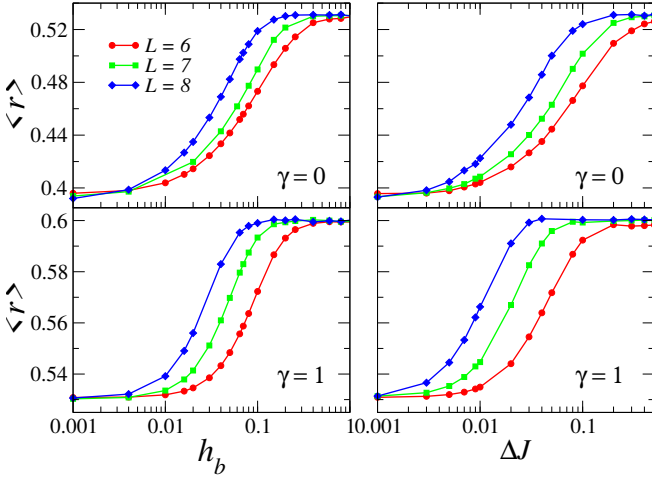


FIG. 3. Mean gap ratio for different system sizes in the delocalized regime ($W = 3$) as a function of the strength of the symmetry breaking local magnetic field (left) or the assumed difference between tunneling rates for spin up and down fermions (right) which also breaks the symmetry. The top row represents TRI case, $\gamma = 0$ where presence of symmetries results in a superposition of independent spectra yielding Poisson-like statistics. For complex fluxes, the residual reflection symmetry between spin up and down fermions (for unit filling) combined with TRI leads to generalized time-reversal symmetry (see discussion in the text) leading to an apparent GOE-like behaviour. Only breaking this symmetry by a local field or difference in tunneling rates, the GUE-like statistics corresponding to broken TRI is observed.

III. SPECTRAL STATISTICS

We consider first the statistical spectral properties of the model. A widely used signature of localization properties of a many-body system is the so called gap ratio statistics [10]. From eigenvalue spectrum of the many-body Hamiltonian one computes the average gap ratio $\langle r \rangle$, where $r_n = \min(\delta E_n, \delta E_{n+1}) / \max(\delta E_n, \delta E_{n+1})$ with E_n being the energy levels and $\delta E_n = E_{n+1} - E_n$ is the spacing between two consecutive eigenvalues. It turns out that the mean gap ratio may be correlated with the localization properties of eigenstates. For a localized system described by the Poisson level statistics, the mean gap ratio is $\langle r_{\text{Poisson}} \rangle = 2 \ln 2 - 1 \approx 0.3863$; whereas the ergodic system is described by $\langle r \rangle$ corresponding to GOE $\langle r_{\text{GOE}} \rangle = 0.5306$ for real Hamiltonian matrix and GUE $\langle r_{\text{GUE}} \rangle = 0.5996$ in the absence of (the generalized) time-reversal symmetry [51]. The mean gap ratio may depends on energy (e.g. for systems with the mobility edge) [11, 52–54] thus it should be determined in the interval of energies where one expects the dynamics to be similar. Thus, from now on, we average r_n over the states lying in the center of the spectrum for which $\epsilon_n \equiv (E_n - E_{\min}) / (E_{\max} - E_{\min}) \approx 0.5$ where E_{\min} and E_{\max} are the smallest and largest eigenvalues for a given disorder realization. Finally we average the obtained r_n over disorder realizations.

Such a mean gap ratio as a function of disorder strength for Hamiltonian (1) is shown in Fig. 2. The on-site interaction is fixed at $U = 1$. Consider first $\gamma = 0$ case - then TRI in

Hamiltonian (1) is preserved. Without the symmetry breaking term, Hamiltonian (2), the individual spectra from diagonalizations consist of independent subsets of eigenvalues due to conserved quantities. Hence, the value of the average gap ratio $\langle r \rangle$ is close to the Poisson value for arbitrary disorder strength W vis. [Fig. 2(a)]. To observe the transition between ergodic and MBL phases, we use the explicit forms of generators of SU(2) symmetry

$$S^z = \frac{1}{2} \sum_j (\hat{n}_{j,\uparrow} - \hat{n}_{j,\downarrow}), \quad S^+ = (S^-)^\dagger = \sum_j \hat{c}_{j,\uparrow}^\dagger \hat{c}_{j,\downarrow} \quad (3)$$

$$S^2 = \frac{1}{2} (S^+ S^- + S^- S^+) + (S^z)^2. \quad (4)$$

For $K = 1$, the total number of up/down fermions, $N_\uparrow / N_\downarrow$ is not conserved and $[H_0, S^z] \neq 0$. However, the Hamiltonian still commutes with $S^x = (S^+ + S^-) / 2$ and S^2 operators as can be checked by a direct calculation. Calculating the Hamiltonian matrix in a basis composed of eigenstates of S^2 and S^x and performing exact diagonalization within a single block of the matrix, we explicitly observe the crossover between ergodic and MBL regimes as demonstrated in the inset of Fig. 2(a).

Alternatively, the crossover can be observed by applying the symmetry breaking local Hamiltonian (2) [26] indeed, as Fig. 2(b) demonstrates at weak W , $\langle r \rangle$ reaches the value $\langle r_{\text{GOE}} \rangle$, while at strong disorder it approaches $\langle r_{\text{Poisson}} \rangle$. This indicates the existence of two phases at $\gamma = 0$.

In order to extract the critical disorder strength W_c and exponent ν of transition we use the finite-size scaling technique. We collapse the curves of different system sizes L as a function of $(W - W_c) L^{1/\nu}$ as shown in the inset of the Fig. 2(b). The critical disorder strength is the value of W at which the curves cross or merge and indicates the ergodic to MBL transition. We estimate $W_c \sim 13.2$ and $\nu \sim 0.8$. Observe that as in the spinless fermions case (equivalent to the spin Heisenberg chain) [11] the critical exponent breaks the Harris bound which is 2 for one dimensional system [55]. In the latter case it has been suggested that the possible explanation may be related to the character of the transition resembling a Kosterlitz-Thouless transition [56] with possible important logarithmic corrections.

The remaining symmetries of Hamiltonian (1) for TRI case ($\gamma = 0$) may be alternatively removed by making the tunneling J spin dependent, i.e. $J_\uparrow = J_\downarrow + \Delta J$. Both cases are visualized in Fig. 3 - top row. At $W = 3$ the system is characterized by almost Poissonian mean gap ratio in the presence of symmetries. The finite value of h_b couples different symmetry classes and reveals the true extended character of the system with $\langle r \rangle$ corresponding to GOE (top left panel). A very similar behavior is observed when spin dependent tunneling is present (top right panel). In both cases the larger the system the smaller value of the symmetry breaking parameter is required to fully break symmetry constraints.

Let us now consider the case of nonvanishing phase γ in tunnelings - compare Hamiltonian (1). Non-zero γ breaks

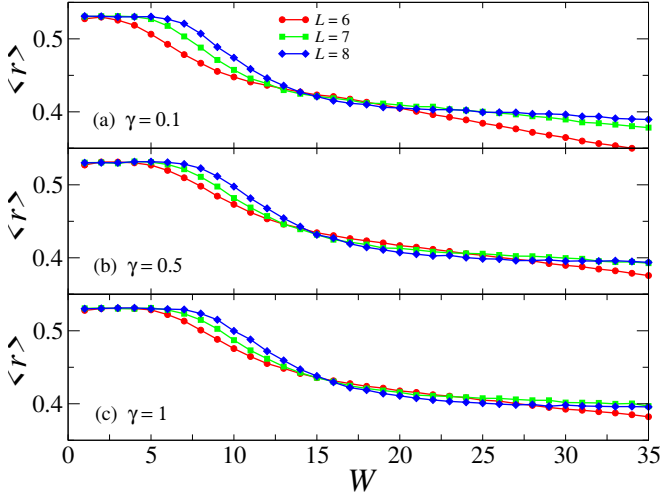


FIG. 4. Transition from GOE-like to Poissonian behavior, i.e. from delocalized to localized regime for Hamiltonian (1) possessing, for $\gamma > 0$, a generalized time reversal symmetry for different values of γ as indicated in the figure. Observe that the crossover point between phases does not depend on γ .

simple TRI - one might naively expect in that case the GUE-like behavior in delocalized regime. Yet, as shown in the bottom row in Fig. 3 without h_b (or spin dependent tunneling) the mean gap ratio $\langle r \rangle \approx 0.53$ points towards GOE statistics. This is explained by the fact that while standard TRI is broken, there exists a generalized TRI in our system (1), namely TRI combined with reflection in $x-y$ plane (i.e. change of the spin direction). That generalized TRI leads to GOE statistics (for an excellent discussion of symmetries in different universality classes see [57]).

With the introduction of h_b or spin dependent tunneling this generalized TRI symmetry is broken and, once the symmetry is fully broken, the GUE statistics is fully recovered in the delocalized regime as shown in the bottom row of Fig. 3.

Consider now the crossover from the delocalized to localized regime for nonzero γ , i.e., in the presence of a synthetic field. Let us discuss first the case with $h_b = 0$ and a generalized TRI - compare Fig. 4. Please note that the observed GOE - Poisson transition in mean gap ratio values seems not to depend on γ (once it is sufficiently big to mix different symmetries). This could in principle be quantified by comparison of finite size scaling parameters obtained - we refrain from such a procedure as the obtained values of W_c must be regarded as only rough estimates due to small system sizes. Thus we rely for this observation on the crossing points of curves in Fig. 4 for different system sizes.

On the contrary, in the presence of additional local field [i.e. adding the term (2) to the Hamiltonian (1)] the transition between GUE and Poisson-like behaviour becomes dependent on γ as apparent from data presented in Fig. 5. One might think that this shift of the transition is related to the way in which the symmetry is broken, namely by a local magnetic field. Such a local perturbation might differently affect the transition to the localized phase for different value of γ . How-

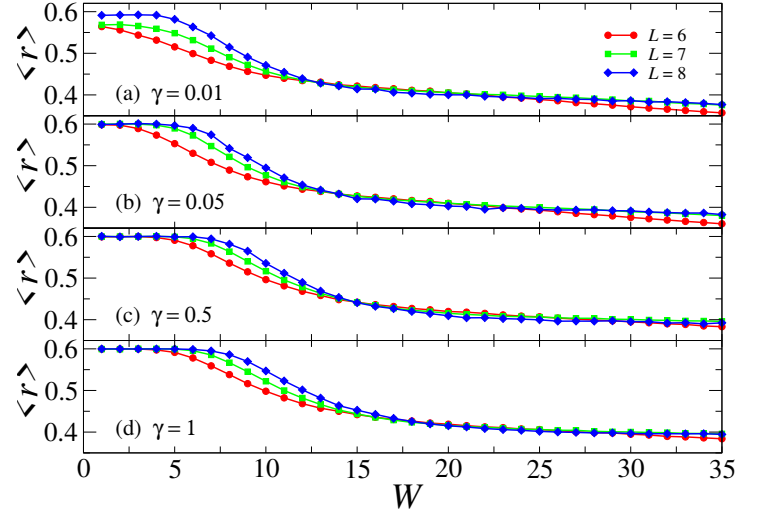


FIG. 5. Transition from GUE-like to Poissonian behavior, i.e. from delocalized to localized regime for Hamiltonian (1) with additional symmetry breaking term (2) with $h_b = 0.5$. Contrary to $h_b = 0$ case presented in Fig. 4 now the crossover point between phases significantly depends on γ .

ever, we have checked, by adding random fields on all of the lattice sites that this is not the case.

IV. DYNAMICS AND DENSITY CORRELATIONS

To study the dynamical properties, we choose random Fock state $|\psi(0)\rangle$ as an initial state for the temporal evolution and examine the dynamics of the local correlations and the entanglement entropy for $L = 8$. The local charge and spin correlations are $C(t) = A \sum_j \langle \rho_j(t) \rho_j(0) \rangle$ and $S(t) = B \sum_j \langle m_j(t) m_j(0) \rangle$, where $\rho_j = n_j - \bar{n}$ with the average density $\bar{n} = \sum_j n_j / L$, and A and B are normalization constant such that $C(0) = S(0) = 1$. Recall that n_j (m_j) are the sum (difference) site occupations of up and down polarized fermions, respectively. We assume a unit filling, $\bar{n} = 1$. The memory of the initial state is lost for ergodic system and this leads to decay of the charge and spin correlations. Interesting situation occurs for the localized phase where (in the absence of symmetry breaking local magnetic field or other effects destroying the system symmetries) the charge sector appears localized but spin sector does not show localization [32, 35]. The absence of fully localized phase is due to the SU(2) symmetry of the model. The choice of a different random potential for up and down polarized fermions, a random magnetic field or a weak spin asymmetry which breaks the SU(2) spin symmetry recovers the full MBL phase [34, 58, 59]. Moreover, the subdiffusive transport of spins is due to a singular random distribution of effective spin exchange interactions [33] and at long time evolution the transport is strongly suppressed [35]. The particle transport rate is exponentially small in J/W , and the rate depends strongly on the initial state of the system. The states occupied with only doublons or holons exhibit full MBL

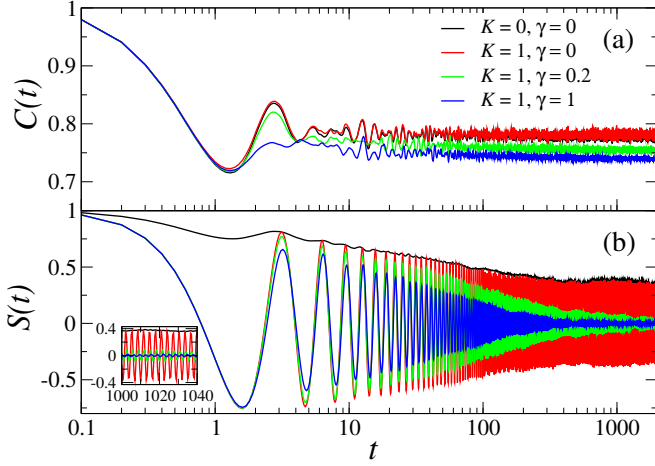


FIG. 6. Time evolutions of the local charge and spin correlations of random Fock states for $U = 1$, $W = 32$ and $h_b = 0$. (a) The charge remains localized in the presence of the synthetic flux. (b) In the absence of the flux, when $K = 0$, the spin delocalizes with subdiffusive decay of correlations. Once K is finite, the spins oscillate (red curve) and the $S(t)$ of $K = 0$ (black curve) provides an envelope to these oscillations. This is apparent from the inset plot where the oscillations in the evolution during large time are concentrated. At $\gamma = 0.2$, the oscillations are damped and $S(t)$ saturates to zero. The damping of the oscillations are pronounced as the flux value increases, as evident for $\gamma = 1$. The gauge field delocalizes the spins. Here, the average over disorder is performed for 300 realizations.

phase as for such states the delocalization rate is zero [36]. This is the current understanding of dynamical properties of disordered Hubbard model. Considering the coupling of spin up and down particles allows for further studies of ergodicity breaking in the model.

We concentrate mostly on the localized side of the transition. The long time evolution of density and spin correlations are shown in Fig. 6. We examine the behaviour of the correlations at several values of the synthetic flux to observe its influence on the dynamics. For $\gamma = 0$, $K = 0$ (i.e. no coupling between the up and down polarized fermions) the charge correlation $C(t)$ saturates at a finite value for an exemplary $W = 32$ value. Also at zero flux ($\gamma = 0$), the coupling of spin degrees of freedom through finite hopping along the synthetic dimension ($K = 1$) does not alter the behaviour of $C(t)$ and the charge remains localized. In the presence of a finite synthetic flux $\gamma = 0.2$ and 1, after a transient time of the order of $1/J$, the charge again seems to saturate. Yet a careful analysis of $C(t)$ reveals a residual very slow algebraic decay, $C(t) \propto t^{-\alpha}$ with $\alpha = 0.004$ for $K = \gamma = 1$ as compared to order of magnitude less α for $\gamma = 0$. This may be due to the fact that at fixed $W = 32$ we are slightly closer to the MBL crossover for $K = \gamma = 1$ than for $K = \gamma = 0$ case. Nevertheless, $\alpha = 0.004$ is significantly smaller than the exponent governing residual decay of imbalance at MBL transition in system of spinless fermions [60, 61] thus we believe that the charge sector of the correlated fermions remains localized in the presence of the synthetic gauge field for a sufficiently strong disorder.

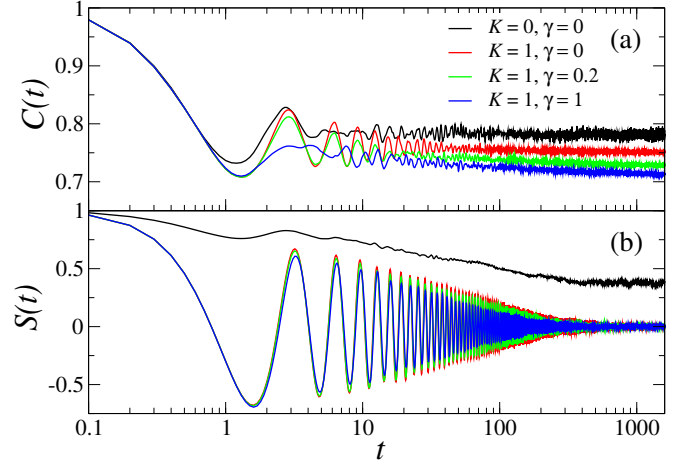


FIG. 7. The local correlations of the hard-core bosons in the localized regime $W = 32$. The initial states are the random Fock states and $U = 1$. (a) The charge is localized in the presence of gauge field. (b) The spins are delocalized, and the spin oscillations saturate to zero at long time evolution. In contrast to the fermionic $S(t)$ [Fig. 6(b)], the spins do not remain oscillatory at $K = 1$, $\gamma = 0$ and the oscillations are damped as time evolves.

Consider now the evolution of the spin correlation $S(t)$ which is shown in Fig. 6(b). In the absence of the flux, the decay of $S(t)$ at long time is suppressed and eventually spins are localized [26, 35]. For $K = 0$ the intermediate time decay of $S(t)$ is monotonic (modulo fluctuations resulting from relatively small number of disorder realizations equal to 300) while the presence of non-zero K leads to oscillations in $S(t)$. The frequency of oscillations is simply K as may be verified in the inset of Fig. 6(b). Interestingly the oscillations have the envelope given by the $S(t)$ curve for $K = 0$. Denoting by H_K the term of H_0 proportional to K and by $H_H = H_0 - H_K$, we verify that $[H_H, H_K] = 0$ as long as $\gamma = 0$. Thus, the evolution operator factorizes: $\exp(-iH_0t) = \exp(-iH_Ht) \exp(-iH_Kt)$ and average number of fermions with spin σ at site j is given by

$$n_{j\sigma}(t) = \langle \psi(0) | e^{iH_Ht} e^{iH_Kt} \hat{n}_{j\sigma} e^{-iH_Kt} e^{-iH_Ht} | \psi(0) \rangle, \quad (5)$$

so that the time evolution of spin correlation function is a superposition of dynamics determined by the H_H Hamiltonian and oscillations driven by the H_K term. The long-time average of the oscillations is zero, which is in agreement with previous study on the localization of coupled chains with correlated disorder [62]. In the presence of a finite flux, $[H_K, H_H] \neq 0$, the oscillations are damped and the damping rate is growing with γ . Thus, the spin sector of the system gets delocalized by the introduction of gauge field.

To examine the effect of quantum statistics, we further analyze the time dependence of local correlations when instead of fermions we consider hard-core bosons in the Hamiltonian (1). The correlations of hard-core bosons for different values of K and γ are shown in Fig. 7. The behaviour of charge correlation, $C(t)$, is similar to the fermionic case and its finite saturation value represents the localization of particles in

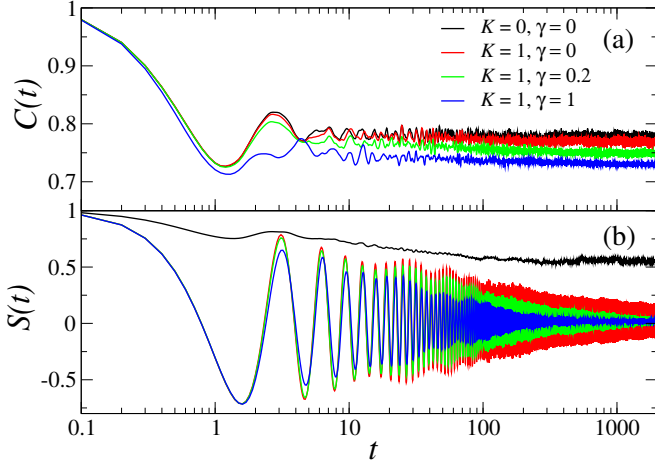


FIG. 8. Same as Fig. 6 but in the additional presence of the local magnetic field term, [Eq.(2)] breaking the generalized TRI symmetry. The influence of coupling K and synthetic flux becomes similar to that of hard-core bosons. The strength of local field $h_b = 0.5$.

the presence of the synthetic flux. The saturation value of $C(t)$ decreases with $0 \leq \gamma \leq 1$ at $K = 1$. The spin sector is localized as $S(t)$ saturates to a finite value when the two hyperfine spin states are decoupled. The coupling of these two states, even for $\gamma = 0$, leads to oscillations, which in contrast to fermionic $S(t)$, are damped to zero. A finite flux γ only weakly affects the damping and spin sector becomes fully delocalized. The stark contrast of $S(t)$ between hard-core bosons and fermions for $K = 1$ and $\gamma = 0$ is a very nice demonstration of effects induced by quantum statistics and different commutation properties of fermions and hard-core bosons (for ground state properties this observation goes back to [63]).

Finally, we return to the fermionic system and calculate time evolution of charge and spin correlation functions as shown in Fig. 8 for non-zero value of symmetry breaking field h_b . In this case, even at $\gamma = 0$ the commutator $[H_H + H_{sb}, H_K] \neq 0$ and the oscillations of $S(t)$ are damped. The effects of broken generalized TRI symmetry, while altering significantly spectral properties of the system, have relatively small effect on time dynamics of correlation functions $C(t)$ and $S(t)$ for $\gamma > 0$.

V. ENTANGLEMENT ENTROPY GROWTH

To corroborate our study of spin delocalization in the presence of the synthetic gauge field we investigate the entanglement entropy growth in the system. The two-leg ladder system can be partitioned in several ways with two prime options: the first version is to cut the ladder perpendicular to the direction of the spatial dimension in two equal (left-right) parts and the second approach is to cut the ladder perpendicular to the direction of synthetic dimension decoupling the hyperfine states. This allows us to study both the entanglement between two left and right ladder subsystems but also between an en-

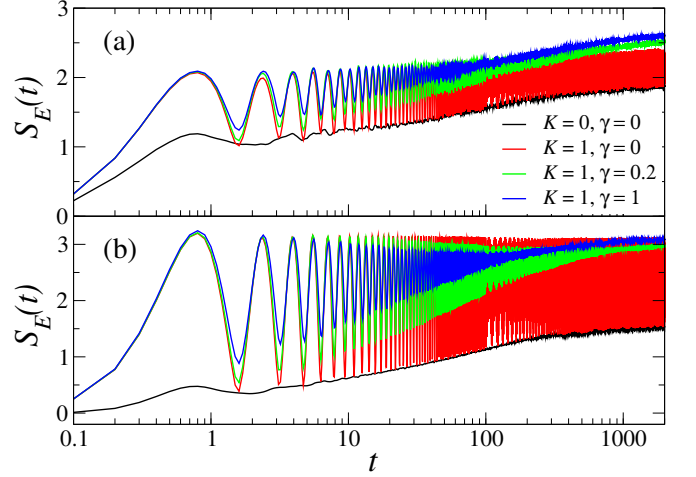


FIG. 9. (a) Left-right bipartite entanglement entropy in the localized regime. With no coupling of spin up and spin down polarized fermions a typical logarithmic growth of S_E is observed after initial transients. Coupling K induces oscillations of the entanglement entropy. Complex flux γ leads to damping of these oscillations with also faster entropy growth. (b) Bipartite entanglement entropy dynamics when rungs of the ladder are cut, i.e. a partition divided up and down polarized fermions.

semble of up and down polarized fermions.

Regardless of the splitting the von Neumann entanglement entropy is defined in a standard way as

$$S_E(t) = -\text{Tr} \rho_A(t) \ln \rho_A(t), \quad (6)$$

where the two subsystems are denoted as A and B with $\rho_A(t) = \text{Tr}_B |\psi(t)\rangle \langle \psi(t)|$ being the reduced density matrix of subsystem A . Here Tr_B is the trace over degrees of freedom of subsystem B .

In the MBL regime the entropy of entanglement of initially separable state should grow logarithmically in time [24, 25] after an initial transient eventually saturating for a finite system size [25]. Such a behavior is indeed observed in our model for decoupled spin chains ($K = \gamma = 0$) both for the standard left-right splitting [Fig. 9(a)] and for the up-down splitting [Fig. 9(b)].

The coupling between up and down polarized fermions introduces strong oscillations in the entanglement entropy, with the same period as revealed by the spin correlation function - compare Fig. 9(a). Similarly, the entropy curve for $K = 0$ forms an envelope (here low lying envelope) to the oscillations. Again this fact is related to vanishing commutators between different kinetic energy terms in the Hamiltonian (1), as described in the previous Section. The presence of complex flux makes these commutators non-zero and introduces the damping of the oscillations. The resulting entropy growth is significantly faster than in the $K = \gamma = 0$ case reflecting the delocalization of spin sector.

Similar, even more spectacular oscillations of the entanglement entropy are observed when the partition divides up and down polarized fermions (i.e. the rungs in the ladder are cut). The coupling between up and down fermions ($K = 1$) makes

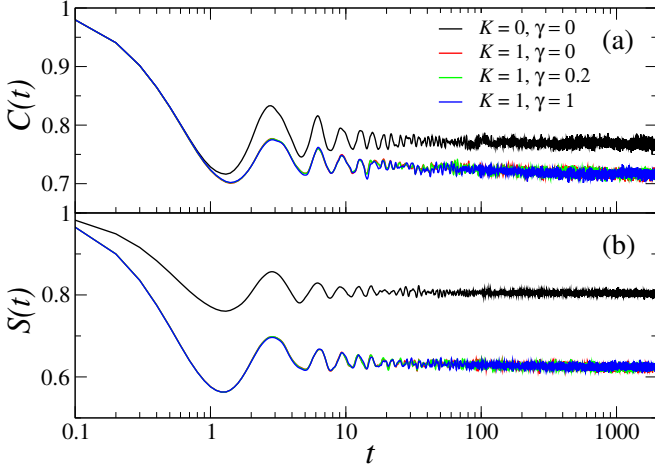


FIG. 10. (a) Charge $C(t)$ and (b) spin $S(t)$ correlation functions for uncorrelated disorder $\epsilon_{j\sigma} \in [-W/2, W/2]$, the chemical potential is site and spin dependent. The system size is $L = 8$, disorder strength $W = 32$, various values of coupling K and flux γ are considered. Both $C(t)$ and $S(t)$ saturate signalling localization of both charge and spin sectors.

the entropy oscillate maximally, with lower envelope given by $K = 0$ curve as before while the upper envelope is system size and disorder strength dependent. Again the non-zero flux introduces damping of these oscillations - on the time scale discussed the entropy growth practically saturates at upper allowed value [Fig. 9(b)].

VI. SPIN-DEPENDENT DISORDER

Up till now we considered the disorder identical for both spin components. Such a situation (albeit for quasiperiodic disorder) is realized in experiments [5]. However, it is possible (and feasible) experimentally to consider a situation when disorder is different (and uncorrelated) for both spin components with the last term in the Hamiltonian (1) changed to $\sum_{j,\sigma} \epsilon_{j,\sigma} \hat{n}_{j,\sigma}$ where now $\epsilon_{j,\sigma}$ are independent random variables drawn from uniform distribution in the interval $[-W/2, W/2]$. The resulting charge and spin correlation functions are shown in Fig. 10. We observe a clear localization of both charge and spin sectors as $C(t)$ and $S(t)$ saturate to constant values after initial oscillations. The fact that addition of a (small amount of) disorder in spin sector, in presence of strong charge disorder is sufficient to fully localize the system was also observed in [59]. The saturation values are lower for $K = 1$ than for $K = 0$ and, interestingly, are independent of the flux γ .

To complete the picture we consider the case of “spin disorder” namely, we replace the last term in Hamiltonian (1) by $\sum_j \epsilon_j (\hat{n}_{j,\uparrow} - \hat{n}_{j,\downarrow})$ so the disorder affects the spin degree of freedom. In this case, for $K = 0$, the system possesses pseudo-spin SU(2) symmetry that can be utilized in studies of its localization properties [64]. Charge and spin correlation functions for various values of K and γ are shown in Fig. 11.

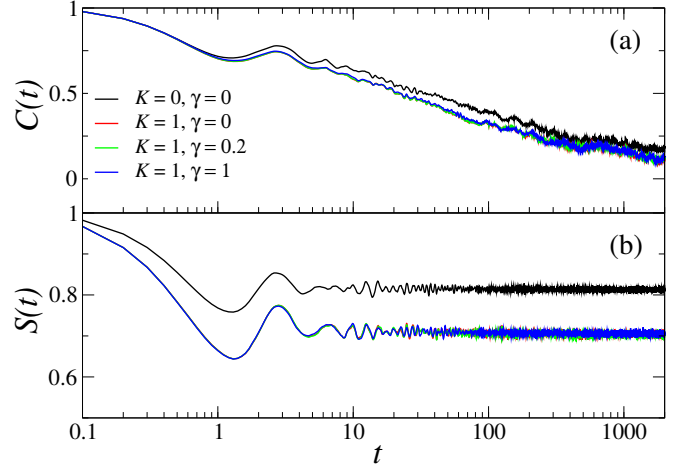


FIG. 11. (a) Charge $C(t)$ and (b) spin $S(t)$ correlation functions for spin disorder $\epsilon_{j\sigma} = -\epsilon_{j\bar{\sigma}}$ (where $\bar{\sigma}$ denotes spin opposite to σ). The system size is $L = 8$, disorder strength $W = 32$, various values of coupling K and flux γ are considered. The saturation of $S(t)$ signals localization of the spin sector whereas the charge sector remains delocalized.

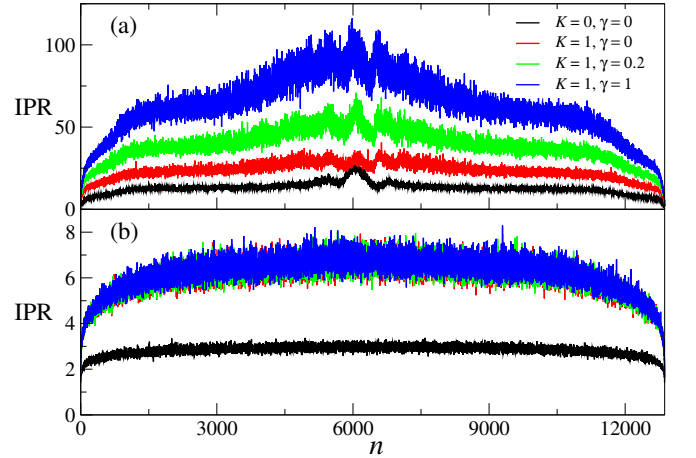


FIG. 12. Averaged over disorder realizations inverse participation ratio (a) for Hamiltonian (1) and (b) for disorder uncorrelated between spin components - leading to full MBL of both charge and spin.

We observe that the spin sector is localized as $S(t)$ quickly saturate whereas the charge correlations decay suggesting delocalization of charge degrees of freedom.

Note that when disorder becomes spin-dependent the time evolution of both charge and spin correlation function is no longer dependent on the phase of the coupling γ between spin components. While for individual realizations of disorder the evolution may differ substantially, the differences average out when taking the disorder average. Once the spin degree of freedom becomes localized the information transfer between the rungs of the ladder stops regardless of γ value. It is worth mentioning that similar independence on the phase of flux is also observed in the entanglement entropy for uncorrelated and “spin disorder”.

One may make this observation even stronger. Consider the

inverse participation ratio of n -th eigenstate $|n\rangle$:

$$\mathcal{I}_n = 1 / \sum_i |\langle n | b_i \rangle|^4, \quad (7)$$

where $|b_i\rangle$ are basis functions (we chose a natural basis of Fock states on lattice sites). We define the averaged over disorder inverse participation ratio as $\text{IPR}(n) = \overline{\mathcal{I}_n}$ with the overbar denoting disorder average. For identical random disorder for both spin components [Hamiltonian (1)] IPR defined in this way depends on K and γ - compare Fig. 12(a). Significant values of IPR indicate that localization is not complete. For the disorder uncorrelated between spin components with the same amplitude W we observe significantly smaller IPR (indicating strong localization), moreover, IPR becomes independent of γ (recall that $\text{IPR}(n)$ are obtained after disorder averaging). Thus not only $C(t)$ or $S(t)$ but also other observables may be expected to be γ -independent once the spin component is localized.

In this respect we observe a clear asymmetry between a real dimension (along the chain) and the synthetic dimension (represented by spin components). The localization of the latter is essential for γ -independence of disorder averaged observables while the charge localization plays little role. Observe that for pure “spin disorder”, as shown in Fig. 11 the correlations for $K = 1$ are flux independent while charge degrees of freedom are delocalized.

VII. CONCLUSIONS

We have analyzed properties of the disordered chain of spin-1/2 fermions in the presence of the synthetic magnetic field. While the spectral properties such as the average gap ratio indicate the transition to many-body localized phase, the time dynamics suggest that MBL is realized in charge (density) sector only. The presence of the synthetic magnetic field delocalizes the spin sector as revealed by the decay of spin time correlation function. Similarly, the entropy of entangle-

ment in the system grows much faster in the presence of the magnetic field flux.

Interestingly the spectral properties of the system strongly depend on the realized symmetries providing a nice example of the effects due to a generalized TRI (i.e. a TRI combined with a discrete symmetry). In effect, despite the standard time reversal symmetry being broken the spectral properties in the delocalized regime resemble that of GOE unless additional symmetry breaking terms are introduced into the model.

A comparison of the dynamics of correlation functions for fermions and hard-core bosons in the absence of the flux ($\gamma = 0$) but when the driving term K couples up and down polarized particles shows sensitivity of the observed phenomena to quantum statistics. For fermions, due to their commutation relations, a kinetic energy part corresponding to the transition between spin up and down fermions commutes with the rest of the Hamiltonian. In effect, the exact quantum dynamics is given by a rapidly oscillating solution whose one envelope is given by $K = 0$ (i.e. no Rabi coupling) solution. This behavior is absent for hard-core bosons.

Last but not least, we considered different types of random disorder, in particular spin dependent disorder that leads to strong localization in the spin sector. In such a case time-dependent observables become, after disorder average, independent of flux γ . We believe that the system sizes examined in present work are sufficient to grasp robust features of considered systems on time scales relevant for experiments with ultracold atoms.

ACKNOWLEDGMENTS

Interesting discussions with T. Chanda, D. Delande and K. Życzkowski on subjects related to this work are acknowledged. The support by PL-Grid Infrastructure was important for this work. This research has been supported by National Science Centre (Poland) under projects 2015/19/B/ST2/01028 (P.S.), 2018/28/T/ST2/00401 (doctoral scholarship – P.S.) and 2016/21/B/ST2/01086 (K.S. and J.Z.).

-
- [1] L. Fleishman and P. W. Anderson, *Phys. Rev. B* **21**, 2366 (1980).
 - [2] F. Alet and N. Laflorencie, *Comptes Rendus Physique* **19**, 498 (2018).
 - [3] S. A. Parameswaran and R. Vasseur, *Reports on Progress in Physics* **81**, 082501 (2018).
 - [4] D. A. Abanin, E. Altman, I. Bloch, and M. Serbyn, *Rev. Mod. Phys.* **91**, 021001 (2019).
 - [5] M. Schreiber, S. S. Hodgman, P. Bordia, H. P. Lüschen, M. H. Fischer, R. Vosk, E. Altman, U. Schneider, and I. Bloch, *Science* **349**, 842 (2015).
 - [6] P. Bordia, H. P. Lüschen, S. S. Hodgman, M. Schreiber, I. Bloch, and U. Schneider, *Phys. Rev. Lett.* **116**, 140401 (2016).
 - [7] P. Bordia, H. Lschen, U. Schneider, M. Knap, and I. Bloch, *Nature Physics* **12**, 907 (2016).
 - [8] J. Smith, A. Lee, P. Richerme, B. Neyenhuis, P. W. Hess, P. Hauke, M. Heyl, D. A. Huse, and C. Monroe, *Nature Physics* **12**, 907 (2016).
 - [9] K. Xu, J.-J. Chen, Y. Zeng, Y.-R. Zhang, C. Song, W. Liu, Q. Guo, P. Zhang, D. Xu, H. Deng, K. Huang, H. Wang, X. Zhu, D. Zheng, and H. Fan, *Phys. Rev. Lett.* **120**, 050507 (2018).
 - [10] V. Oganesyan and D. A. Huse, *Phys. Rev. B* **75**, 155111 (2007).
 - [11] D. J. Luitz, N. Laflorencie, and F. Alet, *Phys. Rev. B* **91**, 081103 (2015).
 - [12] M. Serbyn and J. E. Moore, *Phys. Rev. B* **93**, 041424 (2016).
 - [13] R. Vasseur, A. J. Friedman, S. A. Parameswaran, and A. C. Potter, *Phys. Rev. B* **93**, 134207 (2016).
 - [14] A. Maksymov, P. Sierant, and J. Zakrzewski, *Phys. Rev. B* **99**, 224202 (2019).
 - [15] P. Sierant and J. Zakrzewski, *Phys. Rev. B* **99**, 104205 (2019).
 - [16] P. Sierant and J. Zakrzewski, “Model of level statistics for disordered interacting quantum many-body systems,” (2019),

- arXiv:1907.10336 [cond-mat.dis-nn].
- [17] A. Pal and D. A. Huse, *Phys. Rev. B* **82**, 174411 (2010).
 - [18] M. Serbyn, Z. Papić, and D. A. Abanin, *Phys. Rev. Lett.* **111**, 127201 (2013).
 - [19] D. J. Luitz, N. Laflorencie, and F. Alet, *Phys. Rev. B* **93**, 060201 (2016).
 - [20] P. Sierant, D. Delande, and J. Zakrzewski, *Phys. Rev. A* **95**, 021601 (2017).
 - [21] K. Agarwal, S. Gopalakrishnan, M. Knap, M. Müller, and E. Demler, *Phys. Rev. Lett.* **114**, 160401 (2015).
 - [22] Y. Bar Lev, G. Cohen, and D. R. Reichman, *Phys. Rev. Lett.* **114**, 100601 (2015).
 - [23] M. Kozarzewski, P. Prelovšek, and M. Mierzejewski, *Phys. Rev. B* **93**, 235151 (2016).
 - [24] J. H. Bardarson, F. Pollmann, and J. E. Moore, *Phys. Rev. Lett.* **109**, 017202 (2012).
 - [25] M. Serbyn, Z. Papić, and D. A. Abanin, *Phys. Rev. Lett.* **110**, 260601 (2013).
 - [26] R. Mondaini and M. Rigol, *Phys. Rev. A* **92**, 041601 (2015).
 - [27] J.-y. Choi, S. Hild, J. Zeiher, P. Schauß, A. Rubio-Abadal, T. Yefsah, V. Khemani, D. A. Huse, I. Bloch, and C. Gross, *Science* **352**, 1547 (2016).
 - [28] H. P. Lüschen, P. Bordia, S. Scherg, F. Alet, E. Altman, U. Schneider, and I. Bloch, *Phys. Rev. Lett.* **119**, 260401 (2017).
 - [29] F. A. An, E. J. Meier, and B. Gadway, *Phys. Rev. X* **8**, 031045 (2018).
 - [30] C. Hainaut, I. Manai, J.-F. Clément, J. C. Garreau, P. Szriftgiser, G. Lemari, N. Cherroret, D. Delande, and R. Chicireanu, *Nature Communications* **9**, 1382 (2018).
 - [31] P. Prelovšek, *Phys. Rev. B* **94**, 144204 (2016).
 - [32] P. Prelovšek, O. S. Barišić, and M. Žnidarič, *Phys. Rev. B* **94**, 241104 (2016).
 - [33] M. Kozarzewski, P. Prelovšek, and M. Mierzejewski, *Phys. Rev. Lett.* **120**, 246602 (2018).
 - [34] M. Środa, P. Prelovšek, and M. Mierzejewski, *Phys. Rev. B* **99**, 121110 (2019).
 - [35] J. Zakrzewski and D. Delande, *Phys. Rev. B* **98**, 014203 (2018).
 - [36] I. V. Protopopov and D. A. Abanin, *Phys. Rev. B* **99**, 115111 (2019).
 - [37] Y.-J. Lin, R. L. Compton, K. Jimnez-Garcia, J. V. Porto, and I. B. Spielman, *Nature* **462**, 628 (2009).
 - [38] O. Boada, A. Celi, J. I. Latorre, and M. Lewenstein, *Phys. Rev. Lett.* **108**, 133001 (2012).
 - [39] A. Celi, P. Massignan, J. Ruseckas, N. Goldman, I. B. Spielman, G. Juzeliūnas, and M. Lewenstein, *Phys. Rev. Lett.* **112**, 043001 (2014).
 - [40] L. F. Livi, G. Cappellini, M. Diem, L. Franchi, C. Clivati, M. Frittelli, F. Levi, D. Calonico, J. Catani, M. Inguscio, and L. Fallani, *Phys. Rev. Lett.* **117**, 220401 (2016).
 - [41] C. Cheng and R. Mondaini, *Phys. Rev. A* **94**, 053610 (2016).
 - [42] S. D. Geraedts and R. N. Bhatt, *Phys. Rev. B* **95**, 054303 (2017).
 - [43] J. Major, M. Płodzień, O. Dutta, and J. Zakrzewski, *Phys. Rev. A* **96**, 033620 (2017).
 - [44] D. Suszalski and J. Zakrzewski, *Phys. Rev. A* **94**, 033602 (2016).
 - [45] F. H. L. Essler, H. Frahm, F. Ghmman, A. Klumper, and V. E. Korepin, *The One-Dimensional Hubbard Model* (Cambridge University Press, 2005).
 - [46] S. Zhang, *Phys. Rev. Lett.* **65**, 120 (1990).
 - [47] J. Šuntajs, J. Bonča, T. Prosen, and L. Vidmar, “Quantum chaos challenges many-body localization,” (2019), arXiv:1905.06345 [cond-mat.str-el].
 - [48] D. A. Abanin, J. H. Bardarson, G. D. Tomasi, S. Gopalakrishnan, V. Khemani, S. A. Parameswaran, F. Pollmann, A. C. Potter, M. Serbyn, and R. Vasseur, “Distinguishing localization from chaos: challenges in finite-size systems,” (2019), arXiv:1911.04501 [cond-mat.str-el].
 - [49] P. Sierant, D. Delande, and J. Zakrzewski, “Thouless time analysis of anderson and many-body localization transitions,” (2019), arXiv:1911.06221 [cond-mat.dis-nn].
 - [50] R. K. Panda, A. Scardicchio, M. Schulz, S. R. Taylor, and M. Žnidarič, “Can we study the many-body localisation transition?” (2019), arXiv:1911.07882 [cond-mat.dis-nn].
 - [51] Y. Y. Atas, E. Bogomolny, O. Giraud, and G. Roux, *Phys. Rev. Lett.* **110**, 084101 (2013).
 - [52] S. Nag and A. Garg, *Phys. Rev. B* **96**, 060203 (2017).
 - [53] S.-H. Lin, B. Sbierski, F. Dorfner, C. Karrasch, and F. Heidrich-Meisner, *SciPost Phys.* **4**, 002 (2018).
 - [54] P. Sierant and J. Zakrzewski, *New Journal of Physics* **20**, 043032 (2018).
 - [55] A. Chandran, C. R. Laumann, and V. Oganesyan, (2015), arXiv:1509.04285 [cond-mat.dis-nn].
 - [56] A. Goremkykina, R. Vasseur, and M. Serbyn, *Phys. Rev. Lett.* **122**, 040601 (2019).
 - [57] F. Haake, *Quantum Signatures of Chaos* (Springer, 2013).
 - [58] G. Lemut, M. Mierzejewski, and J. Bonča, *Phys. Rev. Lett.* **119**, 246601 (2017).
 - [59] B. Leijnep-Johns and R. Wortis, *Phys. Rev. B* **100**, 125132 (2019).
 - [60] E. V. H. Doggen, F. Schindler, K. S. Tikhonov, A. D. Mirlin, T. Neupert, D. G. Polyakov, and I. V. Gornyi, *Phys. Rev. B* **98**, 174202 (2018).
 - [61] T. Chanda, P. Sierant, and J. Zakrzewski, (2019), arXiv:1908.06524 [cond-mat.stat-mech].
 - [62] Y. Zhao, S. Ahmed, and J. Sirker, *Phys. Rev. B* **95**, 235152 (2017).
 - [63] F. Crépin, N. Laflorencie, G. Roux, and P. Simon, *Phys. Rev. B* **84**, 054517 (2011).
 - [64] X. Yu, D. Luo, and B. K. Clark, *Phys. Rev. B* **98**, 115106 (2018).